

Study on infrared differential thermal non-destructive testing technology of the permeability of hot mix asphalt pavements

Duanyi Wang¹ and Jicun Shi^{*1,2}

¹Department of Civil Engineering and Transportation South China University of Technology, Guangzhou, Guangdong, China

²Henan Gaoyuan Maintenance Technology of highway CO., Ltd. Xinxiang, Henan, China

Abstract. In order to non-destructive test (NDT) the permeability coefficient of hot mix asphalt (HMA) pavements fast, A methodology for assessing the permeability coefficient was proposed by infrared differential thermal testing of pavement after rain. The relationship between permeability coefficient and air voids of HMA specimen determined. Finite element method (FEM) models were built to calculate the surface temperature difference with different exposure time after precipitation. Simulated solar radiation source and fully saturated plate specimens were set in laboratory, tests verify that the different exposure time the specimen surface temperature difference. Infrared differential thermal detection permeable pavement hardware and corresponding software developed. Based on many test results, the evaluation index and criteria of permeability coefficient of HMA pavements tested by infrared differential thermal were developed. The results showed that: There is correlation between air voids and permeability coefficient of HMA specimen. Permeability coefficient of HMA pavements can be determined by different surface temperature at different exposure time. 9:00 am - 14:00 pm is the best time to detect permeability coefficient by infrared differential thermal NDT. Permeable asphalt pavement permeability can be achieved by infrared detector quickly and continuously, a lane testing; Per the permeable assessment criteria, in-place pavements permeability coefficients can be accurately evaluated.

1 Introduction

Semi-rigid asphalt pavements early distresses are the most typical water damage^[1]. Due to the uneven nature of asphalt concrete, a large area in air voids, natural rainfall will penetrate the asphalt surface and remain in semi-rigid top surface. Many high-speed driving in the role of free water will have a huge grassroots hydrodynamic pressure and erosion^[2,3]. One of the most basic functions of dense-graded HMA pavements surface is to make the asphalt surface layer can be enclosed rain, snow in the infiltration and protect base and subgrade to prevent water damage. Higher percentages of in-place air voids allow water and air to penetrate the pavement, leading to an increased potential for water damage, oxidation, ravelling, and cracking^[4]. Especially with heavy traffic, hydrodynamic asphalt binder will enable the rapid erosion flaking, loss, and can make the semi-rigid embankment liquefaction, damage the pavement structure.

Now permeability coefficient widely used as a test of HMA pavements permeability to moisture. Permeability coefficient tester is the only device on the road test permeability coefficient currently. This reflects the extent and speed of the internal structure of the surface layer in the structure of the surface layer of the water flowing gaps and connectivity status. Permeability detection testers have a



simple, low cost characteristic. The detection efficiency, representativeness and accuracy of test data, data acquisition and processing degree of automation cannot adapt to the rapid detection of road traffic demand, yet to further improvement. We urgent need to develop a fast, Non-destructive, continuous permeability coefficient asphalt testing equipment and to develop appropriate testing methods. Through research prior art, proposed the use of a certain arrangement of infrared sensor continuously detects the temperature difference between the road surface HMA pavement rapid assessments of permeability coefficient.

2 Infrared differential thermal NDT mechanism and permeability coefficient detection

2.1 Mechanism

The prerequisite of HMA pavements permeability coefficient detected by infrared differential thermal non-destructive testing is the pavements surface adequate moisture, and after a time of sunshine, saturated surface dry. As the air voids of HMA pavements are uneven, after natural precipitation the higher percentages of air voids areas will keep more water (see Figure 1), under the sun, these areas are slow evaporation to form low temperature zone; rather lower percentages of air void impermeable surface, evaporation speed, a high temperature region. The use of an infrared sensor installed in many special test vehicles to detect the temperature difference between the surfaces of HMA pavements. If the temperature difference and permeability coefficients are known, this method can be used to evaluate of HMA pavements permeability coefficient.

Through the above analysis, the definition of infrared differential thermal detection technology of HMA pavements permeability: the use of infrared sensors to detect pavements (or specimens) permeable or impermeable by surface temperature difference, with surface temperature difference translated into permeable pavement index to evaluate the pavements (or specimens) nondestructive testing technology permeability coefficient. The quantitative relationships between surface temperature differences and permeability coefficient have been calculated through experiments and numerical simulation.

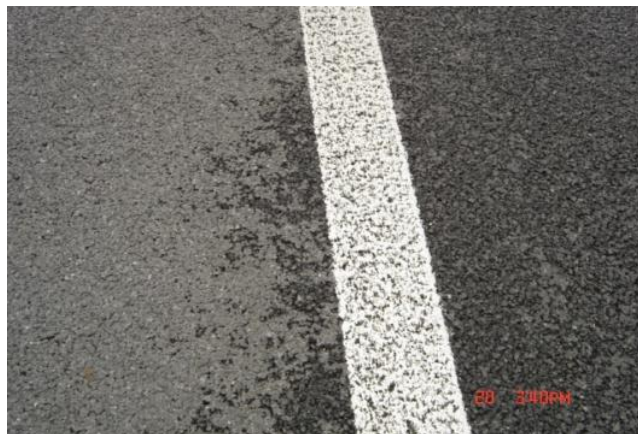


Figure 1: Difference in permeable area with impermeable surface.

At present, there are methods to identify internal distresses by the temperature difference caused by moisture in surface. According common deboned and water distresses of honeycomb structure of aircraft, HUANG heat the specimen actively and detect the specimen information by infrared radiation collecting surface thermal imager, test and finite element calculation results show that the object defects location of cellular water temperature is lower than the temperature of the reference area^[5]; YANG based on mathematical morphology, such as watershed approach enables the identification of defect location and size of the shell-like structure^[6]; WU and other specimens using pulse flash heating by infrared thermography real-time monitoring test meter surface temperature field^[7]. Through the surface temperature difference of specimen to determine the internal defects, enhance and segment thermography image to identify quantitative defects^[8,9,10,11,12].

2.2 Relationship between HMA air voids and permeability coefficient

Laboratory experiments for the study of different permeability coefficient HMA pavement surface temperature, the design of different air voids rut plate specimen to simulate different permeability coefficient. Bitumen is used in the test AH-70, coarse and fine aggregates are limestone, limestone fillers ore, mixture gradation using the AC-16, by adjusting the thickness graded, compacted aggregate ratio and the number of control panels rut the air voids of the specimen. Engineering practice designed air voids was 4.0%, 6.0%, 8.0%, 10.0%, 12.0%, 14.0% of the standard sheet specimen rutting by coring on the specimen to determine the actual air voids of the actual gap rate test results are shown in Table 1.

Table 1: Permeability tests results on rutting specimens.

No.	Target air voids/%	Actual air voids/%	Permeability coefficient $C_w /$ ($\text{mL} \cdot \text{min}^{-1}$)
1	4.0	3.9	43
2	6.0	6.1	80
3	8.0	8.4	126
4	10.0	10.5	355
5	12.0	11.6	537
6	14.0	14.2	768

The relationship between permeability coefficient and air voids of specimen was studied. Permeability tests refer to the standard JTG E60-2008 of T0971-2008 permeability coefficient test method [13]. The results showed that there is a certain correlation between permeability coefficient and air voids of plate specimen, permeability coefficient increases as the air voids of plate specimen. When the actual air voids no more than 8%, it will meet the requirements of surface water permeability coefficient of less than $300 \text{ mL} \cdot \text{min}^{-1}$. Based on the results of this, more plate specimens with different air voids were formed to represent different permeability coefficient.



Figure 2: Permeability tests in laboratory.

2.3 Pavement temperature difference with different permeability calculated by FEM

The FEM model of temperature difference is same with the pavement structure, pavement structure shown in Figure 3. There is a width of 0.4m permeability area set in the middle of the surface layer and other parts are impervious area. Materials parameters related using Reference 3. 24h day of solar radiation through the statistics obtained, calculated by the preparation of the corresponding program.

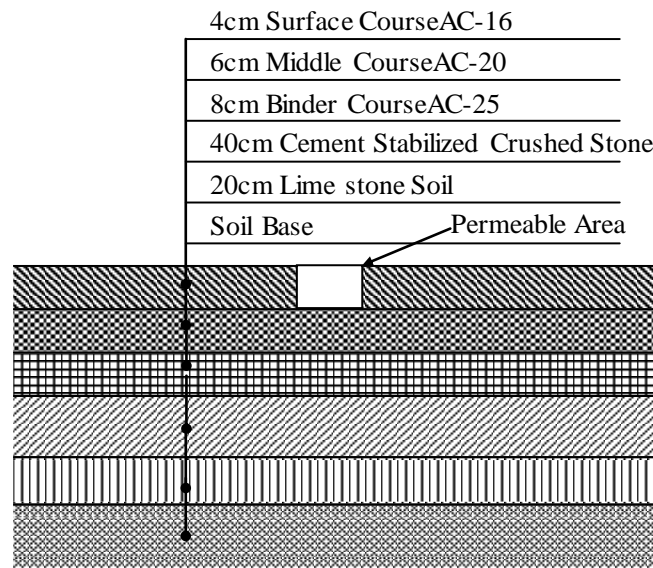


Figure 3: Structure of semi-rigid asphalt Pavement and Permeable Area.

The road surface temperature difference is calculated by FEM and the results shown in Figure 4.

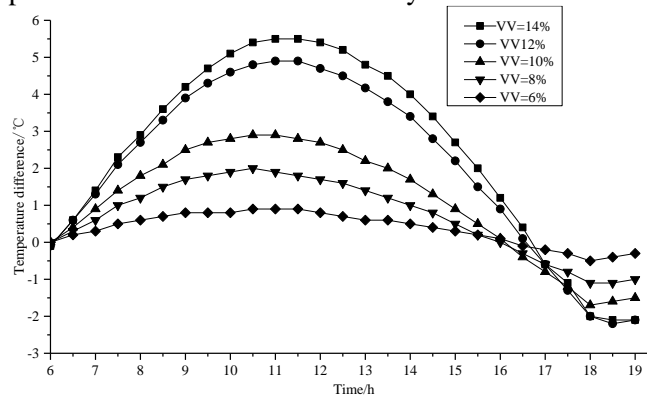


Figure 4: Temperature difference of HMA pavements with different permeability.

By analyzing the FEM results show that: surface temperature differences of impervious and different permeability coefficient road significantly in a day. The maximum temperature differences generally between 11h AM ~ 12hAM. In the same day, with the gradual increase of surface layer permeability, the maximum surface temperature difference of 0.9 °C to 5.7 °C. During 9h AM to 14h PM the road surface temperature differences of heavier permeability sections over 2 °C; Meanwhile solar radiation intensity is reached among the strongest period of the day, generally it is the best opportunity period to evaluate road permeability. 17h in the afternoon, due to the heat release of road surface, temperature difference of road is small, even impervious pavement surface temperature is below the temperature of the permeability area, so it is not recommended at this time to detect road surface permeability coefficient by the road surface temperature difference.

2.4 Experimental study of the relationship between surface temperature difference and permeability coefficient of HMA specimen

First, a plurality of HMA plate specimen with different permeability coefficient and size of 30cm × 30cm × 5cm are made. Next, permeability coefficient of HMA plate specimen is measured, and soaked in water at room temperature no less than 12h. Another, the specimen is placed over the slightly larger metal box, surrounding space sealed with plasticine. Then, the specimen placed under irradiance using the same sources of solar radiation after weighed. Once every 10min weight and surface temperature is measured and recorded. Stop the test until surface temperature of impervious

and permeable specimen not more than 0.5 °C. Surface temperature difference is calculated using equation 1, where both laboratory and field test results are applicable.

$$\Delta T = T_i - T_0 \quad (1)$$

Where, ΔT -specimen (or road) surface temperature difference, °C; T_i - specimen (or road) surface temperature of permeability category i , °C; T_0 - surface temperature of impervious specimen (or road), °C.

To make the indoor and outdoor simulation results are consistent, we use TM-207-type solar radiation meter to detect the day from sunrise to sunset total solar radiation. The northern region of Henan solar radiation illuminance from July to September measured value curve fitting. Halogen lamps are used as indoor simulated solar radiation source. To ensure the test area irradiance uniformity the halogen lamp power, the distance between specimens and lamps, layout positions are designed detailed. Figure 5 is a test surface temperature and permeability coefficient of the specimens.

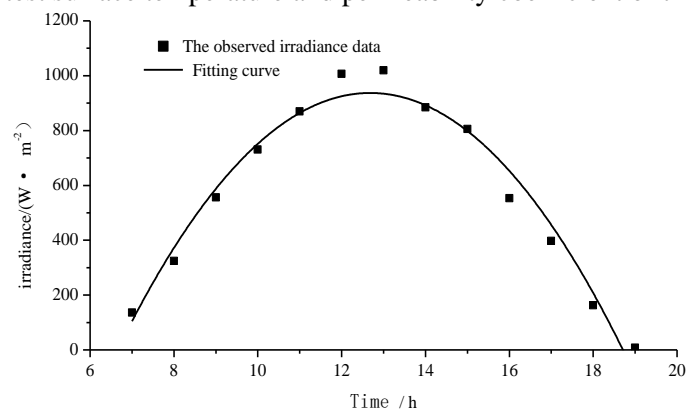


Figure 5: Irradiance curve in one day.



Figure 6: Test of surface temperature and permeability coefficient.

With the time extension of the indoor test, the water in specimen continues to evaporate and the surface temperature difference will gradually decrease. the specimen surface temperature difference change is shown in figure 7. To meet the test requirements of scene, stop test when the temperature difference between impervious and permeable specimen not more than 0.5 °C.

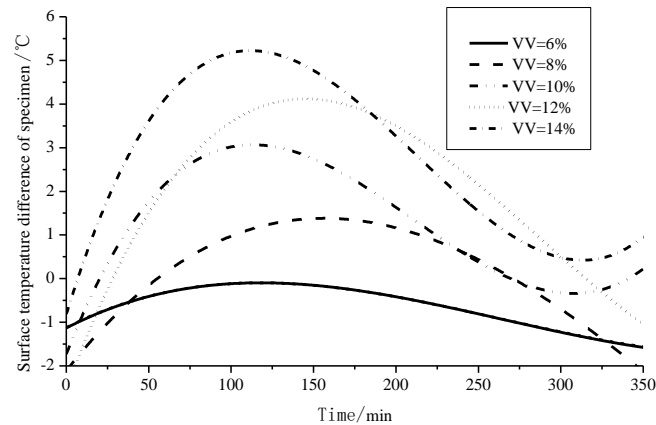


Figure 7: Fitting curve of different surface temperature with different permeability of specimens.

By comparing specimens of different permeability coefficient under the same irradiation conditions analysis showed that the temperature difference of specimens with different permeability coefficient gradually increase and tends to zero, the maximum temperature difference up to 5.7 °C. During the first 30min, the temperature difference is not obvious between the different air voids of the specimen, in general illumination 50min ~ 200min, the temperature difference can reach more than 2 °C, and can be used as a time reference value optimum detection timing. After irradiation the specimen with designed air voids of not less than 8% (i.e. permeability serious) surface temperature difference will be more than 2 °C. In the period of significant temperature difference, the large temperature difference representative major permeability coefficient and small one representative minor.

The specimens with different permeability coefficients are irradiated 1h, 2h, 3h, 4h, 5h, then the temperature difference is analyzed, and the results shown in Fig 8. From the figure results, the greater the surface permeability coefficient greater the temperature difference; if known irradiation time, and through on-site detection of road surface temperature, the surface permeability coefficient can be calculated by the difference between the figure 8 and the corresponding calculation.

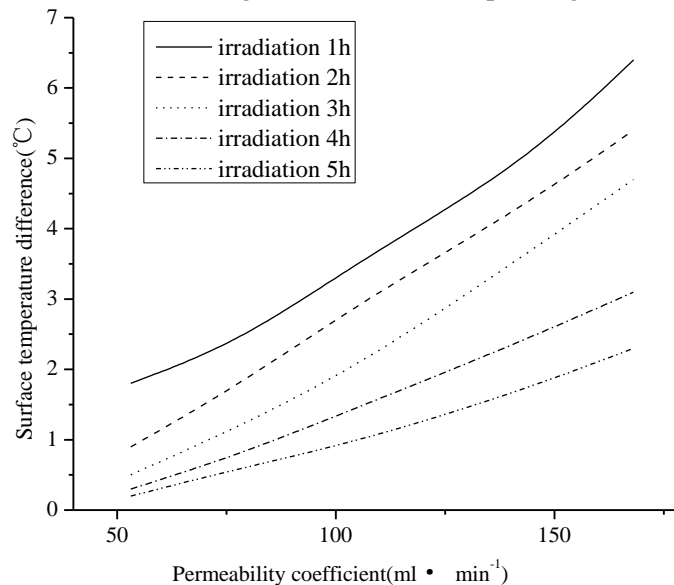


Figure 8: Relationship of the specimen surface temperature and water permeability coefficient.

3 Researches and development on asphalt pavement permeability detector based on differential thermal infrared

Based on the above permeability differential thermal infrared detection mechanism, vehicle-mounted water permeable asphalt pavement detector is developed. The detector can be covering a lane width,

speed reached 100 km/h, temperature measurement error is less than 0.5°C, can adapt to the road scene environment temperature and humidity conditions and vehicle vibration.

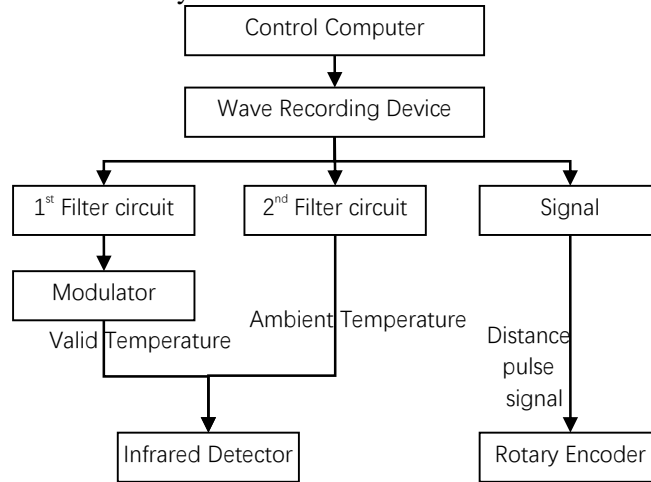


Figure 9: Differential thermal infrared detector schematics.

3.1 Hardware

The hardware consists of pavement temperature acquisition systems by infrared sensor and position system. Eight high-speed response infrared sensors are designed and can cover the entire width of a lane, temperature measurement accuracy less than ± 1 °C. The detector system also has some resistance to the vibration and bump characteristics. To reduce infrared temperature probe wandering, the eight infrared probes require calibration settings using blackbody source. Temperature signals detected by infrared sensors are converted into voltage signals, and by filtering and amplification, the useful signals and the noise signals are distinguished. Position system uses the leine & linde-RS1505 rotary encoder Produced in Switzerland. The rotary encoder is not only able to meet a variety of environmental conditions including rain and bumpy test section etc., and can meet the high speed requirements.

3.2 Software System

HMA pavement surface temperature is detected by infrared temperature measurement system fast and continuous. The event log window is set for keep records of event log files of various external factors pavement temperature at the time of detection. The temperature signal, position information and event data stored in computer are interpreted. Computer's data and curve pattern are formed. Accordance with a predetermined evaluation standard, HMA surface is evaluated permeability levels and the data output a report.



Figure 10: Permeability infrared detector developed.

4 Evaluation and standards of pavement permeability coefficient

The above method can detect the road surface temperature, but many on-site testings showed that the surface temperature difference will be greater volatility with the weather conditions, road conditions, and testing time. The impacts of external factors are eliminated by defining the temperature difference degrees.

$$U = k \frac{\Delta T}{T_0} \times 100\% \quad (2)$$

Where, U- temperature difference degree, %; k- correction coefficient of temperature difference degree, regression from a lot of data, calculated by the formula 3.

$$k = \frac{T - 30}{T^{1.48}} + 1 \quad (3)$$

Through a certain transformation equation, Pavement Water Permeable Index (PWPI) is used for evaluate the pavement permeability coefficient. Formula 4 is the calculation method of PWPI.

$$PWPI = 100 - 2 \cdot U \quad (4)$$

After many roads are detected, the relationship between PWPI and permeability coefficient is regression, the results shown in Fig 11.

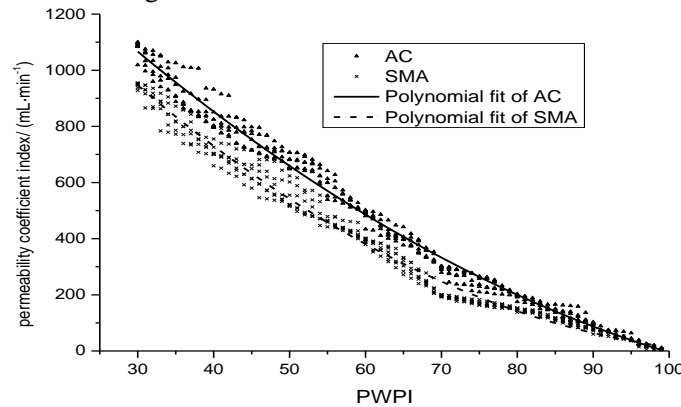


Figure 11: Relationship between permeability coefficient and PWPI.

Through the relationship between permeability coefficient and PWPI, permeability category and standards of HMA pavement are established, as shown in Table 2. According to the evaluation criteria, the same level of surface water permeability coefficient is divided into the same category; assess the level of the corresponding permeability category, permeability regional area.

Table 2 Permeability category and standards of HMA pavement

Permeability category	PWPI	Permeability coefficient of the reference value (mL/min)	
		Dense-graded asphalt concrete	SMA
1	≥90	0~100	0~80
2	≥80, <90	100~200	80~150
3	≥70, <80	200~300	150~200
4	≥60, <70	300~500	200~400
5	<60	≥500	≥400

As can be seen from the above evaluation, the smaller permeability indexes the severe permeability. Grade 3 of PWPI is the threshold to determine the surface water permeability. Using infrared differential thermal method can quickly distinguish the severity level of the road surface permeability, provide the basis for the implementation of the HMA pavement preventive maintenance.

Using the evaluation criteria and methods for freeway G4 (Beijing-Hong Kong-Macau) K641 +421 ~ K663 +134 upstream of the first lane permeability were detected. The road surface layer is dense-graded asphalt concrete. The results are shown in Table 3.

Table 3. Freeway G4 (Beijing, Hong Kong and Macao) K641 +421 ~ K663 +821.

Start stake number	End stake number	PWPI	Category	Permeable area (m ²)
K641+421	K641+821	65	4	1440
K642+750	K642+954	54	5	383
K645+538	K647+220	63	4	6290
K649+396	K650+524	68	4	2645
K651+217	K651+876	65	4	1548
K652+003	K652+136	62	4	205
K654+158	K655+149	67	4	3716
K659+488	K660+014	52	5	1973
K662+221	K662+509	65	4	1288
K663+134	K663+821	62	4	1234

For the detection of permeable sections, fog seal, chip seal, etc. overlay can be used.

5 Conclusions

- (1) There is a positive correlation between air voids and permeability coefficient of HMA pavement; permeability coefficient increases as the air voids; when the measured air voids of plate specimens not more than 8%, it can meet the pavement permeability coefficient of less than the requirements of 300 mL·min⁻¹.
- (2) The temperature difference between the road surface changes with the exposure time, the maximum temperature difference increase from 0.9 °C to 5.7 °C; During 9h AM to 14h PM the road surface temperature differences of heavier permeability sections over 2 °C, generally it is the best opportunity period to evaluate road permeability.
- (3) The designed vehicle-mounted water-permeable asphalt pavement detector can cover a lane width, speed reached 100 km/h, and calculate and output the detection results via software system.
- (4) Test, numerical simulation and field test results analyzed to determine the relationship between permeability coefficient and permeability index, the establishment of a permeable HMA pavement evaluation grade and standards, according the standard to determine the extent of permeable pavement.

Acknowledgements

This work was supported by intergovernmental international cooperation on science and technology innovation of the Ministry of Science and Technology of China (2016YFE0111000) .

References

- [1] WANG, W. et al. Grey Relation Degree Analysis on Influencing Factors of the Permeability of Asphalt Pavements. *Journal of Wuhan University of Technology* **32**, pp. 83-87,(2010).
- [2] DAN, H.C. et al. Evaluation Analysis and Test for Permeability of SMA Pavements. *Journal of Central South University : Science and Technology* **42**, pp. 3536-3544,(2011).
- [3] VARDANEGA, P.J. & WATERS, T.J. Analysis of Asphalt Concrete Permeability Data Using Representative Pore Size. *Journal of Materials in Civil Engineering* **23**, pp.169–176, (2011).
- [4] FENG, D.C. et al. Experimental Study on Permeability Characteristic of Asphalt Mixture. *Journal of Building Materials* **13**, pp. 182-186+209, (2010).
- [5] HUANG, X.P. et al. Thermal Wave Nondestructive Testing of Honeycomb Defects and Finite Element Modeling. *Acta Optica Sinica* **33**, pp. 103-109, (2013).
- [6] YANG, Z.W. et al. Infrared Thermography Applied to Detect Debond Defect in Shell Structure. *Infrared and Laser Engineering* **40**, pp. 186-191, (2011).

- [7] WU C.Q. et al. Infrared Thermography Nondestructive Testing of Debond Defects in Composite Materials. *High Power Laser and Particle Beams* **23**, pp.3271-3274,(2011).
- [8] HAININ, M. R. et al. The Effect of Lift Thickness on Permeability and the Time Available for Compaction of Hot Mix Asphalt Pavement under Tropical Climate Condition. *Construction and Building Materials* **48**, pp.315-324, (2013).
- [9] CAO, D. & QU, H.M. Research on Material Infrared Nondestructive Testing Based on Finite Element. *Laser & Infrared* **43**, pp. 513-517, (2013).
- [10] MAIERHOFER, C. et al. Non-destructive Testing of Cu Solder Connections Using Active Thermography. *NDT and E International* **52**, pp.103-111, (2012).
- [11] HUO, Y. & ZHANG, C.L. Quantitative Infrared Prediction Method for Defect Depth in Carbon Fiber Reinforced Plastics Composite. *Acta Phys. Sin.* **61**, pp.199-205, (2012).
- [12] JIA, L. et al. A Numerical Temperature Prediction Model for Asphalt Concrete Pavement *Journal of Tongji University (Natural Science)* **35**, pp. 1039-1043, (2007).
- [13] MINHOTO, M.J.C. et al. Predicting Asphalt Pavement Temperature with a Three-Dimensional Finite Element Method. *Transportation Research Record* **1919**, pp. 96-110, (2005).